BEAM POSITION AND PHASE MONITORS CHARACTERIZED AND INSTALLED IN THE LANSCE CCL*

J. D. Gilpatrick#, V. Kutac, D. Martinez, R. McCrady, J. O'Hara, F. Olivas, R. B. Shurter, H. Watkins, LANL, Los Alamos, NM, 87544, USA

Abstract

The Los Alamos Neutron Science Center - Risk Mitigation Project is in the process of replacing older Coupled-Cavity-Linac (CCL) Beam-Position Monitors (BPMs) with newer Beam Position and Phase Monitors (BPPMs) and their associated electronics and cable plants. In many locations, these older BPMs include a separate Delta-T loop for measuring the beam's central phase and energy. Thirty-one BPPMs have been installed and many have monitored the charged particle beam. The installation of these newer BPPMs is the first step to installing complete BPPM measurement systems. Prior to the installation, a characterization of each BPPM took place. The characterization procedure includes a mechanical inspection, a vacuum testing, and associated electrical tests. The BPPM electrical tests for all four electrodes include contact resistance measurements, Time Domain Reflectometer (TDR) measurements, relative 201.25-MHz phase measurements, and finally a set of position-sensitive mapping measurements were performed which included associated fitting routines. This paper will show these data for a typical characterized BPPM.

INTRODUCTION

LANSCE-RM is presently installing newer BPPMs and replacing the older BPMs. The older BPMs are in two forms; a device consisting of a short small cavity with four, B-dot loops, and the same four, B-dot loop structure and an additional cylindrical capacitive electrode. All of the older BPMs' signals are connected to a single-ended TNC-connector vacuum feedthru and provide bipolar doublet signals for 201.25-MHz position and phase measurements. Unfortunately, the position measurements provided by the four, B-dot loops are unreliable.

The newer BPPMs differ from the older BPMs in that the BPPMs have a clear aperture whose diameter is the same as the beam pipe immediately upstream of the BPPM. The design of these BPPMs does not perturb the bunched beam image currents traveling along the beam pipe. The BPPMs also use a shorted-upstream electrode design that provides the bipolar doublet signal. Furthermore, the BPPMs 201.25-MHz signal from the summed four electrodes provides a position-independent phase signal. This phase of the summed-electrode BPPM signal uses the CCL beam-cavity phasing and acceleration measurement, locally known as the Delta-T procedure.

Table 1 displays the mechanical details of the newer BPPM. The calculated position sensitivity is based on a simple analytic model of a BPPM and the simulated position sensitivity is based on a MAFIA simulations [1].

The BPPM measurement requirements include the dynamic range and signal-to-noise requirements [2]. These requirements do not include beam debunching that occurs during the phase measurements for the 201.25-MHz Delta-T procedure and are described by another paper at this workshop [3].

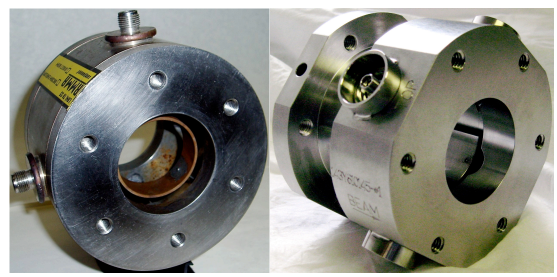

Figure 1: The older BPM (left) shows the inner capacitive Delta-T electrode and a newer BPPM (right) shows a typical inner electrode.

Table 1: Shorted-Upstream-Electrode BPPM Details

Mechanical Characteristics	Value
Electrode Characteristic Impedance (Ω)	50
Electrode Inner Radius (mm)	22.2
Electrode Length (mm)	50.3
Electrode Subtended Angle (degrees)	60
Body Inner Radius (mm)	22.2
Flange-to-Flange distance (mm)	76.2
Simulated Position Sensitivity (dB/mm)	1.26
Simple Calculated Position Sensitivity (dB/mm)	1.50

Additionally, the BPPMs use single-ended SMA vacuum feed-thru connector by CeramTek [4]. A separate physical guard partially protects the connector from external mechanical abuse.

Alignment tooling is added to each BPPM so that they may be observed by a separate Laser Tracking system. Because the BPPM mapper centering mechanism uses the same alignment tooling to center the BPPM as the Laser Tracking system, this alignment technique allows for accurate transverse beam location.

After an initial visual inspection, a vacuum test verified that the individual feed-thru and other vacuum interfaces were operational.

*Work supported by U. S. Department of Energy
#gilpatrick@lanl.gov

ISBN 978-3-95450-121-2

ELECTRODE CONTACT RESISTANCE CHARACTERIZATION

The received 120 feed-thrus manufactured by Ceramtek did not test as expected [4]. The two-finger collets of the input sockets for each vacuum feed-thru (and associated electrode) did not have a low contact resistance of <40 mΩ. After a microscopic visual inspection and a contact resistance measurement, it was discovered that these fingers did not appear to have a bend, i.e., the collet fingers exerted no lateral force on the mating SMA-connector pin. In some cases, there was no contact at all between the feed-thru socket fingers and the mating SMA-connector pin.

To remedy this condition, the collet fingers were bent beyond the yield point using special tools. Their contact resistance and TDR were again measured and operationally verified.

An Agilent 34410A milli-ohm 4-wire resistance measurement was performed on each BPPM-electrode feed-thru received. The final average contact resistance measured for the 112 feed-thrus (2 BPPMs were left unchanged for comparison at a later date) was 23 mΩ and a minimum and maximum resistance of 15 and 33 mΩ, respectively.

ELECTRODE TDR CHARACTERIZATION

Once the contact resistance for each electrode was verified to be small, a TDR was used to determine all electrode impedances. Each BPPM electrode was expected to be manufactured exactly the same. However, due to slight differences in manufacturing, electrode characteristic impedances vary. Figure 2 shows all four BPPM electrodes. Initially, two of the four TDR feed-thrus exhibited larger variations than the other feed-thrus. This was due to the incorrect impedance and resultant contact resistance measurements. While one can observe slight electrode impedance variations and differences, the

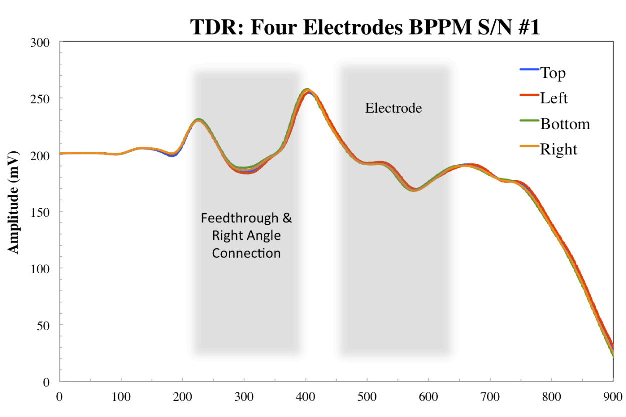

Figure 2: This graph shows the TDRs of all four BPPM feed-thrus, right-angle connections, and electrodes. These plots were acquired after each collet finger was bent resulting in an expected low contact resistance.

TDR shows the four feed-thrus, four right angle connections, and four electrodes having similar approximate impedances.

BEAM POSITION CHARACTERIZATION

The BPPM's were also characterized by acquiring their position offsets, sensitivities, and nonlinear terms using a single-wire mapping facility. On the mapping facility antenna wire, an RF sinusoidal signal resides. As the vertically oriented antenna wire is moved to different transverse BPPM locations, the induced current and resulting signal power are digitized. The BPPMs are then mapped to ~75% of their radius or to ~17 mm on a 1-mm grid. Figure 3 shows a 2-D position sensitivity map.

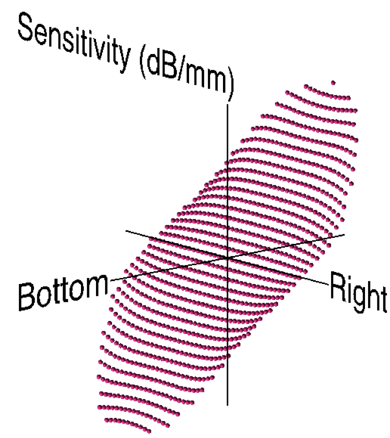

Figure 3: The above graph shows the plot of BPPM vertical sensitivity as a function of relative power and beam location.

Each BPPM is mechanically centered within the mapper facility with its associated flats and optical alignment monuments and then mapped. Using these same alignment monuments, the mapper facility's associated laser system allows a BPPM and the mapper mechanical centers to be aligned to within 0.025 mm.

At each mapper antenna-wire location, the four signal powers were acquired using a Boonton 4-channel Model 4300 RF power meter. The 201.25-MHz signal, from a HP 8640B signal generator, feeds the antenna wire. The beam data includes the calibrated horizontal- and vertical-location coordinates of the antenna wire, and the amount of electrode signal power acquired by each of the four Boonton 51075 RF Power Sensors, and appropriate header data. After these BPPMs were mapped, the mapper and LabVIEW software were rebuilt. The rebuilt mapper facility is described in a paper at this beam instrumentation workshop [5].

The analysis consists of fitting each axis data set with offset, sensitivity, and third-order terms using a 2-D nonlinear polynomial fitting routine. The errors between the fit equation and the actual mapped-BPPM data was observed to be <1% for mapper-wire locations inside 50% of the BPPM's radius and <4% for mapper-wire locations inside 75% of the BPPM's radius.

ISBN 978-3-95450-121-2

Due to each BPPM's manufacturing quality, the error bars were small enough such that the fitting errors did not include the second order terms coefficients. However, the offsets did show an ~+/-0.25 dB variation.

An analytic model for the position sensitivity has been available in the technical literature for some time [6,7,8]. This analytic model assumes a line charged-particle beam modulated at the beam's fundamental-bunching frequency. For the BPPM positional sensitivity, the bunched-beam surface or image charges travel along the four symmetrically spaced electrodes or lobes with known radius and length. The BPPM's transverse position sensitivity may then be expressed as a solution to the Laplace equation for cylindrical boundary conditions. Its sensitivity is the ratio of the right and left electrode signals (e.g., horizontal axis) for these bunched-beam image currents [8]. Because this power ratio is a solved using the Bessel series, this same signal power ratio can be approximated with a four-term or ten-term, 2-D non-linear 3rd-order fitted equation [9].

For the horizontal axis, the four-term forward fitting equation is

$$R_x\left[dB\right] = x_0 + S_x x + S_{3cross} x y^2 + S_3 x^3 , \qquad [1]$$

where R_x,, S_x, S_3, S_{3Cross} are the coefficients of this fitting equation, x and y are the Cartesian coordinates of the mapping wire, x_0 is the fitted offset RF relative power.

The inverse fitting equation is also calculated and provides the sensitivities and etc. to the computer reporting systems.

Table 2 shows the average (Avg) and standard deviations (Stdev) of these values. The positional offsets varied from +0.65 to -0.92 mm but the sensitivities were typically 0.822 mm/dB or 1.19 dB/mm. Both of the BPPMs 3rd-order coefficients were the same within the standard deviation constraints, therefore, only a single value is provided.

Table 2: Based on Position Mapping Data, Details of 38 Manufactured BPPMs

BPPM Fit Coefficients	Avg	Stdev
Offset, Hor. (dB)	-1.8×10^{-4}	0.28
Offset, Ver. (dB)	8.9×10^{-4}	0.23
Sensitivity, Hor. (dB/mm)	1.19	0.0047
Sensitivity, Ver. (dB/mm)	1.19	0.0048
3rd-Order Coef., Hor., (dB/mm^3)	-1.8×10^{-4}	5.0×10^{-6}
3rd-Order Cross Coef., Hor., (dB/mm^3)	3.5×10^{-4}	5.0×10^{-6}

PHASE CHARACTERIZATION

Since these BPPM's are used to measure the linac-cavities phase and amplitude set points, a phase characterization was also performed. These bench measurements verify each electrode's phase delay expected during both the injected "self test" mode and beam phase measurements. The measurement test jig includes a transformation from the outer shield radius of an RF N-connector to the BPPM 22.2-mm inner-bore radius. This transformation test jig maintains and is terminated in 50-Ω characteristic impedance. The BPPM-electrode signal power is obtained using an S_{21} measurement from an Agilent Technologies E5070B Network Analyzer.

The phase delay characteristics were measured at the fundamental bunching frequency (201.25 MHz), and the 1st and 3rd harmonics. All electrodes had a measured absolute phase delay spread of < 1.8, 201.25-MHz-deg. The transmission-line-to-electrode attenuation for all electrodes was between -27 and +/-0.4 dB, and again, within bench and beam line measurement tolerances.

SUMMARY

Thirty-one of the characterized BPPMs have been installed and many CCL BPPMs are operating as expected. By measuring the BPPMs' feed-thru contact resistance, performing electrode TDR's, mapping each of the BPPM's position sensitivities, offsets and 3rd-order coefficients, and measuring each BPPM's electrode phase delay, thirty-eight BPPMs have been characterized. After some initial minor difficulties, we corrected the BPPM contact resistance such that all of the contact resistance and TDR measurements operated as expected. The BPPM's position sensitivity is 1.19 dB/mm with offsets of ~0.25 dB. The absolute phase delays are spread of <1.8, 201.25-MHz-deg and within bench and beam line measurement tolerances.

REFERENCES

[1] S. Kurennoy, "Electromagnetic Modeling of Beam Position and Phase Monitors for LANSCE Linac," PAC, Albuquerque, NM, pp. 4111-4113 (2007).

[2] J. D. Gilpatrick, et al., "Proposed Beam Position and Phase Measurements for the LANSCE Linac," DIPAC'07, Venice, pp. 78-80 (2007).

[3] R. McCrady, "Beam Position and Phase Monitors for the LANSCE Linac," this workshop.

[4] Ceramtek Part # 8071-02-W, http://www2.ceramtec.com/ .

[5] Heath Watkins, "Beam Position and Phase Monitor - Wire Mapping System," this workshop.

[6] J. H. Cuperous, "Monitoring of Particle Beams at High Frequencies," **NIM**, 145, pp. 219-231, 1977.

[7] R. E. Shafer, "Characteristics of Directional Coupler Beam Position Monitors," IEEE Transactions on Nuclear Science. Vol. NS-32, No. 5, pp 1933-1937, October 1985.

[8] J. D. Gilpatrick, et al., "Experience with the Ground Test Accelerator Beam-Measurement Instrumentation," AIP Conference Proceedings 319, pp. 154-169, 1993.

[9] J. Power, et al., "Characterisation of Beam Position Monitors in Two Dimensions," 1992 Linear Accelerator Conference Proceedings, Attawa. August 1992, pp. 362–364.

ISBN 978-3-95450-121-2